



CO Oxidation Activities of CeO₂ Film Tailored by Loquat Leaves†

JUNCHAO QIAN^{1,2}, CHENGBAO LIU^{1,3}, FENG CHEN³, ZHIGANG CHEN^{1,3,4,*}, YUZHU ZHANG² and MENG MENG WANG²

¹Jiangsu Key Laboratory for Environment Functional Materials, Suzhou University of Science and Technology, Suzhou 215009, P.R. China

²Jiangsu Key Laboratory for Photon Manufacturing, Jiangsu University, Zhenjiang 212013, Jiangsu Province, P.R. China

³School of Chemistry, Biology and Materials Engineering, Suzhou University of Science and Technology, Suzhou 215009, P.R. China

⁴Jiangsu Provincial Key Laboratory for Interventional Medical Devices, Huaiyin Institute of Technology, Huai'an 223003, Jiangsu Province, P.R. China

*Corresponding author: E-mail: czg@mail.usts.edu.cn

Published online: 1 March 2014;

AJC-14776

A novel loquat leaves based scaffold was adopted for the fabrication of hierarchically biomorphic CeO₂ film with special porous structure *via* incorporating Ce ions into membrane. Scanning electron microscopy, transmission electron microscopy, X-ray diffraction, X-ray photoelectron spectroscopy and nitrogen adsorption-desorption measurements were used to characterize the products. Owing to its ultrathin film, biomorphic CeO₂ film exhibits a high catalytic activity in CO oxidation. This facile strategy may open a new avenue towards replicating desired biological structures for metal oxide catalyst in other potential applications.

Keywords: Biotemplate, Loquat leaf, CO oxidation, CeO₂, Oxygen vacancy.

INTRODUCTION

Many efforts have been directed toward research into shape-control nanostructured mesoporous materials owing to the fact that such materials present superior properties at the nanoscale¹⁻³. Especially, biomimicking nanostructures become the focus of numerous studies, which received considerable attention in the rapidly growing field of catalyst, sensor, electronics and water treatment⁴⁻⁶. Biotemplating is the process of microcellular assembly by replica of natural morphology, where the microstructural features of the biotemplate are retained^{7,8}. Different biotemplates with distinct pore species were used to produce biomorphic materials such as wood⁹, pollen¹⁰, kelp¹¹ and cotton fibers¹².

Ceria-based materials find important applications in solid fuel cells, oxygen storage components for catalysts, UV absorbers and sensors because of the high mobility of the oxygen species and the partial reduction of Ce⁴⁺ to Ce³⁺ which leads to the creation of oxide vacancies in bulk which derive from its fluorite-type structure¹³⁻¹⁵. The delicate hollow structures of natural materials offer significant resource for replication to prepare porous ceria materials.

We have recently described the use of loquat leaves as template to produce porous CeO₂ film by adopting cerium(III)

nitrate [Ce(NO₃)₃·6H₂O] to infiltrate into the plant membrane subsequently the template was removed after calcining. Finally, the as-prepared porous biomorphic CeO₂ film has been employed as catalyst for CO oxidation and exhibited an excellent catalysis activity performance.

EXPERIMENTAL

All reagents used in the experiment were analytically pure and purchased from China National Medicines Corporation Ltd. The loquat leaves were picked from Dongshan Town in Suzhou.

Synthesis: The loquat leaves were washed with ultrapure water and dried at 40 °C for several times. 2.5 g of [Ce(NO₃)₃·6H₂O] was added into 200 mL solution and stirred vigorously. 2 g of loquat leaves were dropped into the precursor solution, obtained by mixing the Ce(NO₃)₃ solution and 50 mL alcohol. During the process of magnetic stirring, the plant membrane can adsorb the Ce ions. As the soaking finished, the plant membrane was taken out followed by centrifugation and washing with ultrapure water for several times. After dried overnight in a clean bench, the template was removed by high temperature calcination (550 °C) for 2 h to obtain biomorphic CeO₂ film.

†Presented at The 7th International Conference on Multi-functional Materials and Applications, held on 22-24 November 2013, Anhui University of Science & Technology, Huainan, Anhui Province, P.R. China

Catalyst characterization: Powder X-ray diffraction (PXRD) measurement was performed on a Rigaku X-ray diffractometer with CuK_α radiation (Rigaku, D/max-RB). The surface structure of the biomorphic CeO₂ sample was studied by using a Field Emission Scanning Electron Microscope (FESEM) model S-4800. The distribution of biomorphic ceria nano-particles was investigated by using a JEM 2100 high resolution transmission electron microscopy (HR-TEM). The distribution of biomorphic CeO₂ film nano-particles was further investigated by using a JEM 2100 high resolution transmission electron microscopy (HR-TEM).

CO Catalytic testing: The catalytic tests were conducted in a temperature-programmed reaction system equipped with a mass chromatography (GC 950 system) for product analysis in a typical reaction, 150 mg product was loaded in a quartz reactor and was heated from room temperature to 800 °C at a heating rate of 2 °C/min. The gas flow amounted to 40 mL/min was composed of 5 % O₂ and 1 % CO with N₂ as balance.

RESULTS AND DISCUSSION

The morphology of CeO₂ replica of loquat leaf has been shown in Fig. 1a. The external surface is characterized by the presence of a considerable number of stars and sphere spaced in a nearly regular way. The stars and sphere decorated on the film present regular diameter and variable lengths, as can be observed in Fig. 1b. Some of these spheres are empty. Moreover, HRTEM demonstrated irregular ceria polycrystals with grain size arranged from 6-10 nm composed of the film. The SAED pattern, showed in Fig. 1d, confirmed the calcined product consists of ceria nanoparticles with a polycrystalline structure.

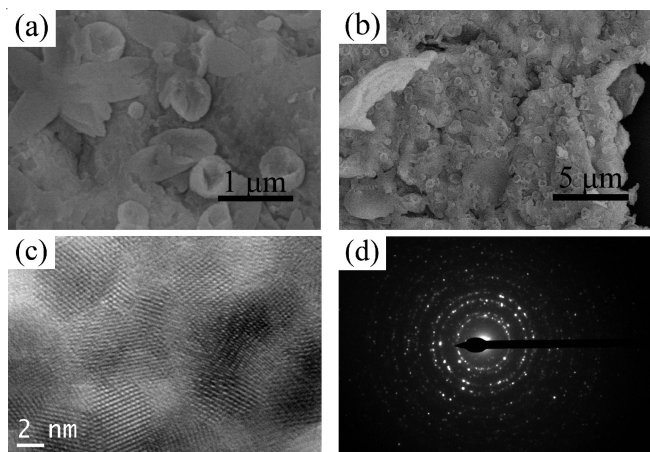


Fig. 1. FESEM micrographs of (a) (b) the CeO₂ replica for the loquat leaf (under different magnification) (c) the High resolution TEM (HRTEM) image of the biomorphic CeO₂ film (d) corresponding selected area diffraction pattern

Fig. 2 shows the XRD patterns of the CeO₂ microspheres. All diffraction peaks in curve could be well indexed as the face-centered cubic pure phase of CeO₂ (JCPDS card No. 34-0394)¹⁶ and the peaks of ceria are remarkably broadened (Fig. 2), implying a significant distortion of the lattice. The crystallite sizes of the as-prepared nanoparticles were calculated by using the Scherrer formula. The sample calcined at 550 °C has a crystallite size of 8 nm.

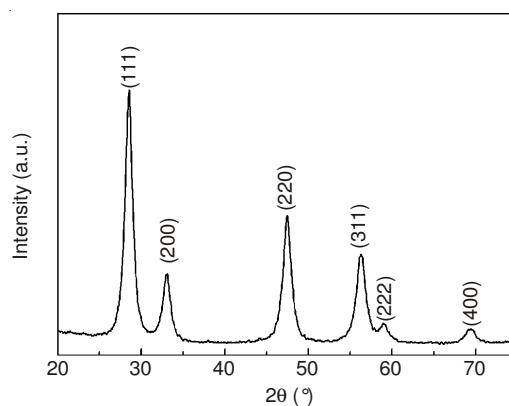


Fig. 2. XRD patterns of biomorphic CeO₂ film

Fig. 3 shows the nitrogen adsorption and desorption isotherms for the CeO₂ film. The porous CeO₂ sample pertained to a typical IV curve with a H3-type hysteresis loop, which implied the characteristic of mesopores according to the IUPAC classification. The specific surface area of the porous ceria film is 82.3 m²/g.

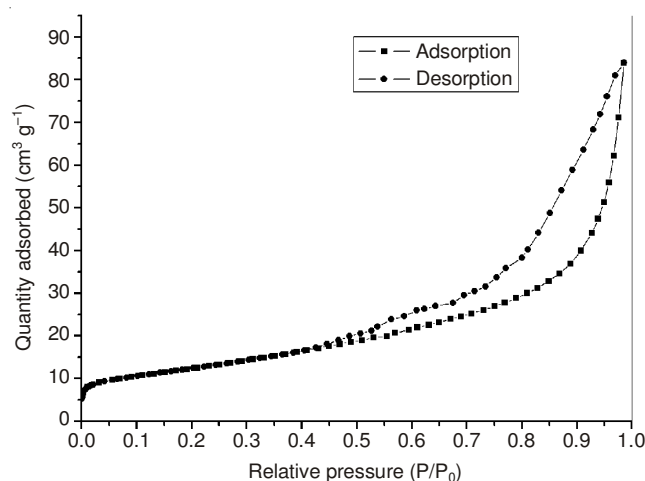


Fig. 3. Nitrogen adsorption-desorption isotherm of biomorphic ceria film

Fig. 4 shows the corresponding pore size distribution curve, a pore diameter distribution within the range of a mesopore (2-50 nm) was observed in the picture. These mesoporous structure further increased the specific surface area of the resulting products, therefore an enhanced catalytic properties was obtained.

Fig. 5 shows the catalytic performance for CO oxidation over the biomorphic ceria film and a reference bulk ceria sample. Compared to the bulk products, the CO conversion of ceria film at ca. 320 °C was above 90 % and a 100 % CO conversion was achieved at 410 °C. The T₅₀ of the biomorph replica is 250 °C while it is 430 °C for the bulk ceria, indicated a great enhancement in catalytic performance of the resulting ceria fibers. Besides the increased specific surface areas, the porous structure is also believed to provide sufficient space for the adsorption of O₂ gas molecular.

Conclusion

In summary, biomorphic ceria film has been successfully synthesized by using the scape of loquat leaves as template.

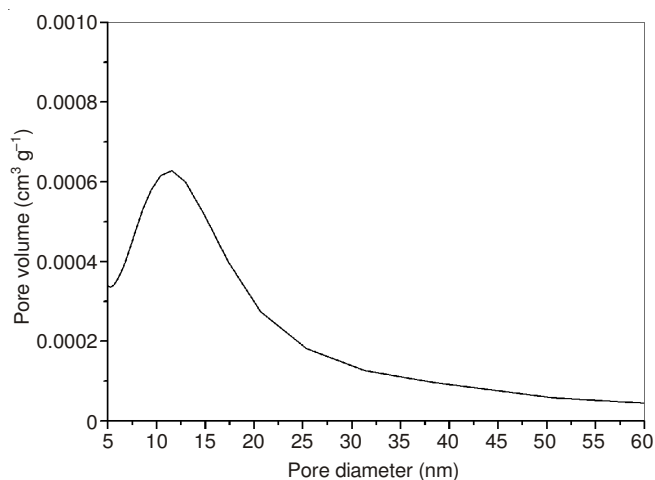


Fig. 4. Corresponding pore size distribution curve of biomorphic ceria film

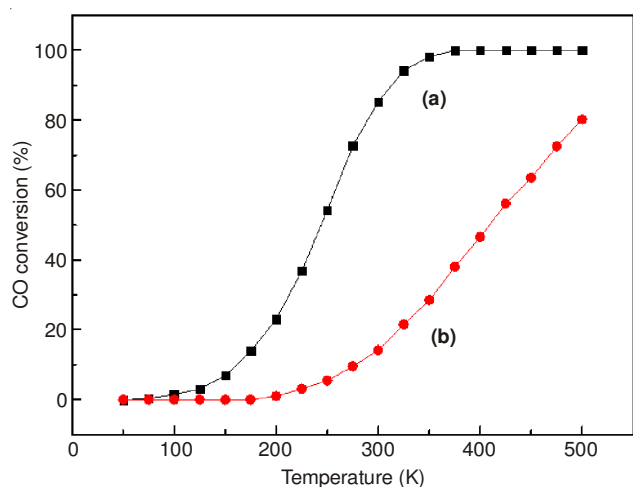


Fig. 5. Catalytic activity of biomorphic ceria film (a) and (b) bulk ceria

The structure of products was comprised of crystallites with grain size 6 to 10 nm. The synthesized materials showed an enhanced surface oxygen activity, as has been discussed by H_2 -TPR analysis. The products also displayed a superior catalytic activity for CO oxidation. For the synthesized fibrous ceria, the CO conversion at 410 °C was 100 % CO, suggesting its potential in auto-gas purification catalysis.

ACKNOWLEDGEMENTS

National Natural Science Foundation of China (21071107, 21277094, 21103119); Production and Research Collaborative Innovation Project of Jiangsu Province (BY2012123); Natural Science Foundation of Jiangsu Province (BK2012167); Science and Technology Pillar Program (Industry) of Jiangsu Province (BE2012101); Collegiate Natural Science Fund of Jiangsu Province (12KJA430005, 11KJB430012); A Project Funded by the Priority Academic Program Development of Jiangsu Higher Education Institutions (PAPD); Applied Basic Research Project of Suzhou (SYG201242, SYG201316); Jiangsu Key Laboratory of Material Tribology (Kjsmcx2011001); Jiangsu Key Laboratory for Photon Manufacturing (GZ201111); Jiangsu Provincial Key Laboratory for Interventional Medical Devices (Jr1210); Science and Technology Pillar Program (Industry) of Changzhou (CE20120067); Creative Project of Postgraduate of Jiangsu Province (CXLX12_0635); Youth project of Suzhou University of Science and Technology (XKQ201213).

REFERENCES

1. X.W. Lou, L.A. Archer and Z. Yang, *Adv. Mater.*, **20**, 3987 (2008).
2. P. Innocenzi, L. Malfatti and G.J.A.A. Soler-Illia, *Chem. Mater.*, **23**, 2501 (2011).
3. S.G. Rudisill, Z. Wang and A. Stein, *Langmuir*, **28**, 7310 (2012).
4. B.D. Briggs and M.R. Knecht, *J. Phys. Chem. Lett.*, **3**, 405 (2012).
5. R. de la Rica and H. Matsui, *Chem. Soc. Rev.*, **39**, 3499 (2010).
6. S. Guo and S. Dong, *J. Mater. Chem.*, **21**, 16704, (2011).
7. T.-X. Fan, S.-K. Chow and D. Zhang, *Progr. Mater. Sci.*, **54**, 542 (2009).
8. S. Sotiropoulou, Y. Sierra-Sastre, S.S. Mark and C.A. Batt, *Chem. Mater.*, **20**, 821 (2008).
9. J.-M. Qian and Z.-H. Jin, *J. Eur. Ceram. Soc.*, **26**, 1311 (2006).
10. S.R. Hall, V.M. Swinerd, F.N. Newby, A.M. Collins and S. Mann, *Chem. Mater.*, **18**, 598 (2006).
11. N. Shi, X. Li, T. Fan, H. Zhou, J. Ding, D. Zhang and H. Zhu, *Energy Environ. Sci.*, **4**, 172 (2010).
12. S. Zhu, D. Zhang, J. Gu, J. Xu, J. Dong and J. Li, *J. Nanopart. Res.*, **12**, 1389 (2010).
13. G.N. Vayssilov, A. Migani and K. Neyman, *J. Phys. Chem. C*, **115**, 16081 (2011).
14. B. Yan and H. Zhu, *J. Nanopart. Res.*, **10**, 1279 (2008).
15. Z. Yang, J. Wei, H. Yang, L. Liu, H. Liang and Y. Yang, *Eur. J. Inorg. Chem.*, 2006 (2011).
16. S.K. Tadokoro, T.C. Porfirio, R. Muccillo and E.N.S. Muccillo, *J. Power Sources*, **130**, 15 (2004).